NeuroImage: Clinical 18 (2018) 51–59

Contents lists available at ScienceDirect

NeuroImage: Clinical

journal homepage: www.elsevier.com/locate/ynicl

Fixel-based analysis reveals alterations is brain microstructure and macrostructure of preterm-born infants at term equivalent age

Kerstin Pannek[a,*], Jurgen Fripp[a], Joanne M. George[b], Simona Fiori[c], Paul B. Colditz[d], Roslyn N. Boyd[b], Stephen E. Rose[a]

[a] Australian E-Health Research Centre, CSIRO, Brisbane, Australia
[b] The University of Queensland, Queensland Cerebral Palsy and Rehabilitation Research Centre, Faculty of Medicine, Brisbane, Australia
[c] IRCCS Fondazione Stella Maris, Pisa, Italy
[d] The University of Queensland, UQ Centre for Clinical Research, Faculty of Medicine, Brisbane, Australia

ARTICLE INFO

Keywords:
Fixel-based analysis
Diffusion
Prematurity
Neonate

ABSTRACT

Preterm birth causes significant disruption in ongoing brain development, frequently resulting in adverse neurodevelopmental outcomes. Brain imaging using diffusion MRI may provide valuable insight into microstructural properties of the developing brain. The aim of this study was to establish whether the recently introduced fixel-based analysis method, with its associated measures of fibre density (FD), fibre bundle cross-section (FC), and fibre density and bundle cross-section (FDC), is suitable for the investigation of the preterm infant brain at term equivalent age. High-angular resolution diffusion weighted images (HARDI) of 55 preterm-born infants and 20 term-born infants, scanned around term-equivalent age, were included in this study (3 T, 64 directions, b = 2000 s/mm^2). Postmenstrual age at the time of MRI, and intracranial volume (FC and FDC only), were identified as confounding variables. Gestational age at birth was correlated with all fixel measures in the splenium of the corpus callosum. Compared to term-born infants, preterm infants showed reduced FD, FC, and FDC in a number of regions, including the corpus callosum, anterior commissure, cortico-spinal tract, optic radiations, and cingulum. Preterm infants with minimal macroscopic brain abnormality showed more extensive reductions than preterm infants without any macroscopic brain abnormality; however, little differences were observed between preterm infants with no and with minimal brain abnormality. FC showed significant reductions in preterm versus term infants outside regions identified with FD and FDC, highlighting the complementary role of these measures. Fixel-based analysis identified both microstructural and macrostructural abnormalities in preterm born infants, providing a more complete picture of early brain development than previous diffusion tensor imaging (DTI) based approaches.

1. Introduction

Preterm birth occurs at a critical time during brain development. Exposure to the extra-uterine environment causes disturbances in the balance of developmental processes of apoptosis, synaptogenesis, and myelination (Volpe, 2009). Infants born prematurely are therefore at an increased risk of motor, cognitive, and behavioural problems (Allen et al., 2011; Saigal and Doyle, 2008). Earlier identification of infants at high risk of developing adverse outcomes would enable earlier, targeted intervention.

Diffusion magnetic resonance imaging (MRI) can provide unique insights into the microstructural development of the brain. Diffusion tensor imaging (DTI) is the most commonly used diffusion MRI method in neonates. Typical measures obtained from DTI include fractional anisotropy (FA), mean diffusivity (MD; sometimes also referred to as apparent diffusion coefficient, ADC), and axial and radial diffusivity. During early brain development, ongoing processes of fibre organisation, membrane proliferation, and (pre-)myelination are thought to impact the DTI measures (Dubois et al., 2008). Indeed, previous studies have shown that DTI measures vary across the lifespan (Hasan et al., 2008; Lebel et al., 2012), with rapid increases in FA and decreases in MD over the first few weeks and years of life (Braga et al., 2015; Kidowaki et al., 2016; Kersbergen et al., 2014; Nossin-Manor et al., 2013; Akazawa et al., 2015). Furthermore, regional patterns of brain development can be observed with DTI (Rose et al., 2014; Wu et al., 2017).

A major limitation of DTI, however, is its inability to resolve crossing fibres. It has been shown previously that between 63 and 90%

* Corresponding author.
E-mail address: kerstin.pannek@csiro.au (K. Pannek).

https://doi.org/10.1016/j.nicl.2018.01.003
Received 14 September 2017; Received in revised form 8 December 2017; Accepted 6 January 2018
Available online 11 January 2018

Table 1
Acquisition parameters.

Contrast	Sequence	Details
T2	HASTE	Acquired in axial, coronal, and sagittal; TR/TE 2000/101 ms; in-plane resolution 0.56 × 0.56 mm; slice thickness 4.8 mm
T2 (quantitative)	Multi-echo TSE axial	TR/TE1/TE2/TE3 10,580/27/122/189 ms; in-plane resolution 0.70 × 0.70 mm; slice thickness 2 mm
T1	MPRAGE	TR/TE/TI 2100/3.18/1500 ms; resolution 1.3 × 1.25 × 1.25 mm
T1	TSE axial	TR/TE 1490/12 ms; in-plane resolution 0.7 × 0.7 mm; slice thickness 2 mm
Perfusion	EPI axial	TR/TE/TI1/TI2 3427.5/21/700/1800 ms; in-plane resolution 4.0 × 4.0 mm; slice thickness 5 mm
Field map	GRE axial	TR/TE1/TE2 488/4.92/7.38 ms; in-plane resolution 2.5 × 2.5 mm; slice thickness 3.25 mm
Diffusion (DTI)	EPI axial	TR/TE 9500/130 ms; 30 directions; b = 1000 s/mm^2; in-plane resolution 1.75 × 1.75 mm; slice thickness 2 mm
Diffusion (HARDI)	EPI axial	TR/TE 9500/130 ms; 64 directions; b = 2000 s/mm^2; in-plane resolution 1.75 × 1.75 mm; slice thickness 2 mm

of white matter voxels in the adult human brain contain crossing fibres (Jeurissen et al., 2013). High angular resolution diffusion weighted imaging (HARDI), in conjunction with advanced models of reconstruction, can be used to overcome this limitation by estimating multiple fibre orientations within each voxel. Today, HARDI is still primarily used to improve the delineation of white matter pathways using tractography, and only rarely to examine local microstructural features in preterm-born infants (Eaton-Rosen et al., 2015; Shi et al., 2016; Gao et al., 2016).

In the current work, we employ a recently developed statistical analysis technique for HARDI data, termed fixel based analysis (FBA; (Raffelt et al., 2016)). A “fixel” describes the different fibre bundles (with different orientations) that may be present within a voxel (Raffelt et al., 2015). Akin to DTI, where each voxel contains information about local FA, MD, and other measures, each fixel carries microstructural (or macrostructural) information which, in contrast to DTI voxels, is specific to the fibre orientation in question. The fixel metrics fibre density (FD), fibre-bundle cross-section (FC), and a combined measure of fibre density and cross-section (FDC) were introduced by Raffelt et al. (2016).

These metrics are thought to provide insight into the different mechanisms that can lead to an alteration in a connection's ability to relay information. A reduction in the total number of axons, according to Raffelt et al. (2016), can manifest in 3 different ways: a) through changes in tissue microstructure (i.e. fewer axons per voxel, however occupying the same spatial extent), b) through changes in tissue macrostructure (i.e. the same number of axons per voxel, however occupying a decreased spatial extent), and c) through a combination of the former two (i.e. fewer axons per voxels occupying a decreased spatial extent). Changes in tissue microstructure (case a) are reflected in the measure fibre density (FD), which is a surrogate marker of the intra-axonal restricted compartment of a fibre bundle. In contrast, fibre-bundle cross-section (FC) refers to the cross-sectional area that is occupied by a fibre bundle, and measures changes in local tissue *macrostructure* (case b). During early brain development, both tissue microstructure and macrostructure change markedly and in conjunction (case c), which can be assessed using the combined measure of fibre density and bundle cross-section (FDC).

Our aim was to establish the utility of FBA in preterm-born infants scanned at term equivalent age (TEA). We investigated (i) whether FD, FC, and FDC are correlated with postmenstrual age (PMA) at the time of MRI and gestational age (GA) at birth; (ii) whether differences in preterm-born infants compared to term-born infants in these measures can be observed; and (iii) whether these differences are more pronounced in the presence of mild macroscopic brain abnormality.

2. Materials and methods

2.1. Participants

Participants for this study were selected from a larger project investigating neurodevelopmental outcomes following very preterm birth (George et al., 2015). Preterm infants born at < 31 weeks completed gestation, admitted to the Royal Brisbane and Women's Hospital Neonatal Intensive Care Unit between January 2013 and April 2016 were eligible for recruitment. Infants were excluded if known genetic or chromosomal abnormality was present, their parents or caregivers did not speak English, or they lived > 200 km from the hospital. A reference sample of healthy term-born infants was also recruited. Term-born infants were eligible if they were born between 38 and 41 weeks gestation following an uncomplicated pregnancy and delivery, had a birth weight above the 10th percentile, were not admitted to the neonatal intensive or special care units, and had a normal neurological examination at the time of the MRI.

The study was approved by the Human Ethics Research Committees at the Royal Brisbane and Women's Hospital (HREC/12/QRBW/245) and The University of Queensland (2012001060).

2.2. MRI

Magnetic Resonance Imaging was performed using a 3 T Siemens TIM Trio (Siemens, Erlangen, Germany). Infants were scanned during natural sleep without sedation, using an MR compatible incubator with a dedicated 8-channel neonatal head coil (Lammers LMT, Lübeck, Germany). Neuroimaging was performed around 30 weeks post-menstrual age and again term equivalent age, and included T1- and T2-weighted structural imaging, multi-echo T2-weighted imaging for estimation of quantitative T2, perfusion imaging, diffusion tensor imaging (DTI; 30 directions, b = 1000 s/mm^2), high angular resolution diffusion weighted imaging (HARDI; 64 directions, b = 2000 s/mm^2), and a field map to assist in the correction of susceptibility distortions on the diffusion images. Acquisition parameters are detailed in Table 1. If signal dropouts were observed during the acquisition of the DTI or HARDI data, acquisition was repeated in the same session when possible. For the current analysis, only structural and HARDI data acquired around term equivalent age were used.

2.3. Scoring of structural images

Structural images were scored by a child neurologist with training in MRI radiology (SF) using the semi-quantitative scoring system of Kidokoro et al. (2013) with modified cut-points for regional measurements (George et al., 2017). The scoring system assesses the domains of white matter, cortical grey matter, deep grey matter, and cerebellum. Scores for a subset of infants included in this study have been presented previously (George et al., 2017). For the current study, only infants with a global score ≤ 3 (indicating none or minimal brain abnormality) were included. The preterm infant group was further subdivided into groups of infants with a global score of 0 (indicating no abnormality in any of the domains), and a global score of 1–3 (indicating mild-to-moderate brain abnormality in at least one of the domains).

2.4. Diffusion image processing

Diffusion data were visually inspected, and datasets were excluded if they contained spike artefacts. Volumes containing motion between

the odd and even subvolumes of the interleaved acquisition were automatically detected using a registration-based approach (Pannek et al., 2017) and removed from further analysis. In cases where multiple repeats of the HARDI data were acquired, the repeat with the best image quality was selected and, when possible, any remaining volumes with head motion in this repeat were replaced with those of the other repeat (s). Datasets containing > 10 rejected volumes were excluded.

Preprocessing of diffusion images included denoising (Manjón et al., 2013), correction for head motion using rigid registration, correction for susceptibility distortions using the field map, removal of non-brain tissue, detection and replacement of signal intensity outliers prior to resampling (Pannek et al., 2012; Morris et al., 2011) and removal of intensity inhomogeneities. Note that denoising was used only to improve registration accuracy; all other corrections were carried out on the original data.

To perform fixel-based analysis, overall image intensity was normalised across subjects using the median b = 0 intensity within white matter. The single fibre response function was estimated after intensity normalisation for each subject using the "Tournier" algorithm implemented in MRtrix (Tournier et al., 2012) (www.mrtrix.org). A group response function was calculated by averaging all individual response functions. Preprocessed diffusion weighted images were upsampled by a factor of 2, and fibre orientation distributions (FOD) were estimated using constrained spherical deconvolution (Tournier et al., 2007), implemented in MRtrix.

A study specific, unbiased FOD template was generated from a subset of infants (10 preterm-born and 10 term-born, selected randomly), using linear and non-linear registration of the FOD images (Raffelt et al., 2011), Fig. 1. Every subject's FOD image was subsequently registered to this template (Raffelt et al., 2011; Raffelt et al., 2012).

Fixel measures of fibre density (FD), fibre cross-section (FDC), and a combined measure of fibre density and cross-section (FDC) were calculated in template space using MRtrix (Raffelt et al., 2016).

2.5. Statistical analysis

Fixel-based statistical analysis was carried out using MRtrix. An analysis mask was created by applying a threshold of 0.33 on the average FOD amplitude. Measures of Fibre Cross-section (FC) were log-transformed prior to statistical analysis, as described previously (Raffelt et al., 2016). Correction for multiple comparisons was performed using connectivity-based fixel enhancement (Raffelt et al., 2015) with 5000 permutations.

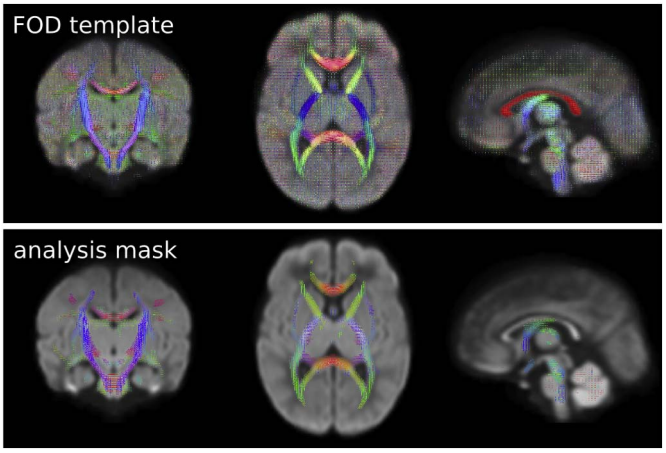

Fig. 1. FOD template and analysis mask. Top: A study specific FOD template was generated from 10 preterm and 10 term infants (selected randomly). Bottom: fibre density, fibre cross-section, and fibre density and cross-section metrics were statistically analysed for fixels with an FOD amplitude exceeding 0.3. Note that fixels perpendicular to the plane of view are not visible (e.g. in the corpus callosum in mid-sagittal view). Colour indicates the orientation of the FOD/fixel orientation (red: left-right, blue: inferior-superior, green: anterior-posterior). (For interpretation of the references to colour in this figure legend, the reader is referred to the web version of this article.)

The following analyses were performed:

- correlations in preterm-born infants:
  - with postmenstrual age at the time of MRI. We hypothesise that PMA at the time of MRI has a global effect on FD, FC, and FDC, indicating ongoing processes of maturation.
  - with estimated intracranial volume at the time of MRI. In their work in adults, Raffelt et al. used the estimated intracranial volume as a nuisance covariate for FC and FDC (but not FD) to remove global effects of brain scaling resulting from the registration to a template (Raffelt et al., 2016). In a neonatal population, intracranial volume is strongly related to postmenstrual age. Therefore, we explicitly investigated whether intracranial volume constituted a confounding variable that was not already accounted for by postmenstrual age. Intracranial volume was estimated indirectly using the brain masks obtained during preprocessing: brain masks were transformed non-linearly to the study-specific template space using the transformations obtained from the FOD registration, the overlap of brain masks of all subjects was calculated, and this mask back-transformed to the individual subject's space for volume estimation. This process ensured that inaccuracies of the individual brain masks did not impact the estimates of intracranial volume; however, we acknowledge that brain volumes may be underestimated due to the required overlap of all brain masks.
  - with gestational age at birth. We hypothesise that the degree of prematurity impacts on white matter microstructure; specifically, we hypothesise that there will be a positive correlation between GA and FD, FC, and FDC in the same brain regions where differences between preterm-born and term-born infants are identified (see below).
- group comparisons:
  - between preterm-born infants (with or without brain abnormality in any of the domains), and term-born infants. We hypothesise that preterm-born infants will show delayed maturation and/or injury of the white matter compared to term-born infants, which will manifest as reduced FD, FC, and FDC in the preterm group.
  - between preterm-born infants *without* brain abnormality in any of the domains, and term-born infants. We hypothesise that differences between preterm-born and term-born infants will be present even in the absence of brain abnormality, which will manifest as reduced FD, FC, and FDC in the preterm group.
  - between preterm-born infants *with* brain abnormality in any of the domains, and term-born infants. We hypothesise that preterm-born infants with brain abnormalities will have greater white matter differences compared to term born infants, than preterm-born infants without brain abnormality, which will manifest as more extended reductions in FD, FC, and FDC.
  - between preterm-born infants with and without brain abnormalities in any of the domains. We hypothesise that preterm-born infants with minimal brain abnormalities on structural imaging will show reductions in FD, FC, and FDC compared to preterm infants without brain abnormality.

We found that PMA at the time of MRI has a profound effect on microstructural measures (see Results section); therefore, PMA was used as a confounder in all analyses. FC and FDC were found to be influenced by brain volume (see Results section), which was therefore included as an additional confounder in the statistical analysis of these measures.

The splenium of the corpus callosum emerged as an important structure in the above analyses (see Results section). To depict correlations and group differences in detail, we manually delineated the

splenium of the corpus callosum on the midsagittal plane, and extracted average measures of FD, FC, and FDC for the primary fibre orientation.

3. Results

3.1. Participants

A total of 105 preterm and 21 term born infants underwent MRI at term equivalent age as part of the prospective cohort study (George et al., 2015). In the current work, we included only infants with a global MRI classification of "normal" based on structural imaging (63 preterm and all term born infants). Data obtained of 8 preterm infants were excluded due to motion artefacts (> 10 volumes removed). Data of 1 term-born infant were excluded due to intrauterine growth restriction. Therefore, 55 preterm (36 male, 19 female, GA at birth 23^{+6}–30^{+6} weeks) and 20 term born infants (12 male, 8 female, GA at birth 38^{+2}–41^{+3} weeks) were included in the analysis. Infants underwent MRI between 38^{+3} and 44^{+6} weeks PMA. While all infants had a global MRI classification of "normal", 26 preterm-born and 2 term-born infants were classified as having mild or moderate abnormalities in at least one of the domains (WM, deep GM, cortical GM, cerebellum) of the scoring system. Here, we consider infants with mild or moderate abnormalities in any of the domains as "minimal abnormality" group, while other infants are considered the "no abnormality" group.

By design, preterm infants were born at younger GA and with lower birth weight than term infants. There was no statistically significant difference in PMA at time of MRI between preterm and term infants ($p = .143$, Wilcoxon's test), and between preterm infants with and without brain abnormality ($p = .761$, Wilcoxon's test). Preterm infants with minimal brain abnormality were born at slightly younger GA ($p = .084$, Wilcoxon's test) and with lower birth weight ($p = .028$, Wilcoxon's test) than preterm infants without brain abnormality. There was no statistically significant difference in the number of removed volumes for included infants; however, more preterm infants than term infants were removed entirely from the analysis due to excessive motion.

Demographics are summarised in Table 2. Detailed information for all participants is provided in Supplementary materials.

3.2. Correlation with postmenstrual age and intracranial volume

Fibre density (FD), FC, and FDC were positively correlated with postmenstrual age (PMA) at the time of MRI and intracranial volume (ICV) throughout the white matter (Fig. 2). The correlation between FC and FDC, and ICV remained statistically significant throughout the white matter after correction for PMA, while the correlation between FD and ICV was statistically significant only in the left posterior limb of the internal capsule, cerebral peduncle, cerebellar peduncle, and anterior commissure. In all further analysis, PMA was therefore considered a confounding variable. In addition, for FC and FDC analyses, ICV was included as a confounding variable.

3.3. Correlation with gestational age

Fibre density (FD), FC, and FDC were positively correlated with GA at birth only in the splenium of the corpus callosum. This relationship remained statistically significant when correcting for PMA and ICV (Fig. 3). The correlation was more widespread and demonstrated lower p-values for FD and FDC, than for FC. A scatter plot visualising the association between fixel metrics and GA at birth is provided in Supplementary Fig. 1, for a region of interest drawn on the midsagittal splenium of the corpus callosum.

3.4. Effect of prematurity and brain abnormality

Results of the group comparisons between preterm and term infants, as well as preterm infants with and without brain abnormality are shown in Fig. 4. Example plots for a region of interest drawn in the splenium of the corpus callosum are provided in Supplementary Fig. 1.

3.4.1. Preterm versus term infants

Fibre density (FD) was significantly reduced in preterm infants compared to term-born infants within the anterior commissure, the fornix bilaterally, the genu of the corpus callosum extending bilaterally to the prefrontal lobe, the midbody of the corpus callosum, and the splenium of the corpus callosum extending bilaterally to the occipital and temporal lobes. The FDC was decreased within the same structures except the anterior midbody of the corpus callosum and the anterior commisure. Furthermore, FC was decreased in preterm infants in the genu of the corpus callosum extending to the prefrontal lobes bilaterally, and the splenium of the corpus callosum. Reductions in FC were also observed in the optic radiations bilaterally (more extensive in the left hemisphere), the cingulum bundle within the temporal lobes bilaterally, the cerebral and cerebellar peduncles bilaterally, the white matter of the right postcentral gyrus, and part of the left superior longitudinal fasciculus.

3.4.2. Preterm subgroups

The preterm infant group was divided into two groups based on presence or absence of minimal brain abnormalities on structural MRI.

3.4.2.1. Fibre density (FD). In preterm infants *without* any brain abnormality compared to term-born infants, FD was reduced in the genu, midbody, and splenium of the corpus callosum, and a small area

Table 2
Demographics.

	Term	Preterm		
		All	No abnormality	Minimal abnormality
n (male/female)	20 (9/11)	55 (19/36)	29 (9/20)	26 (10/16)
GA at birth [weeks^{+days}][a]	39^{+3} (38^{+2}–41^{+3})	28^{+5} (23^{+6}–30^{+6})	28^{+0} (24^{+3}–30^{+6})	29^{+0} (23^{+6}–30^{+6})
Birth weight [grams][a]	3500 (2932–3940)	1188 (584–1886)	1243 (584–1886)	1035 (598–1649)
PMA at MRI [weeks^{+days}][a]	40^{+6} (39^{+2}–42^{+4})	40^{+5} (38^{+3}–44^{+6})	40^{+5} (38^{+3}–42^{+1})	40^{+4} (38^{+6}–44^{+6})
ICV at MRI[a]	511.0 (455.6–540.6)	508.6 (382.6–651.1)	511.2 (446.7–651.0)	490.8 (382.6–651.1)
MRI classification (normal/mild/moderate/severe)				
WM	20/0/0/0	52/3/0/0	29/0/0/0	23/3/0/0
dGM	20/0/0/0	44/8/3/0	29/0/0/0	15/8/3/0
cGM	19/1/0/0	48/2/5/0	29/0/0/0	19/2/5/0
cerebellum	19/1/0/0	45/9/1/0	29/0/0/0	16/9/1/0
global	20/0/0/0	55/0/0/0	29/0/0/0	26/0/0/0

GA: gestational age; PMA: postmenstrual age; MRI: magnetic resonance imaging; ICV: intracranial volume; WM: white matter; dGM: deep grey matter; cGM: cortical grey matter.
[a] Reported are median and range.

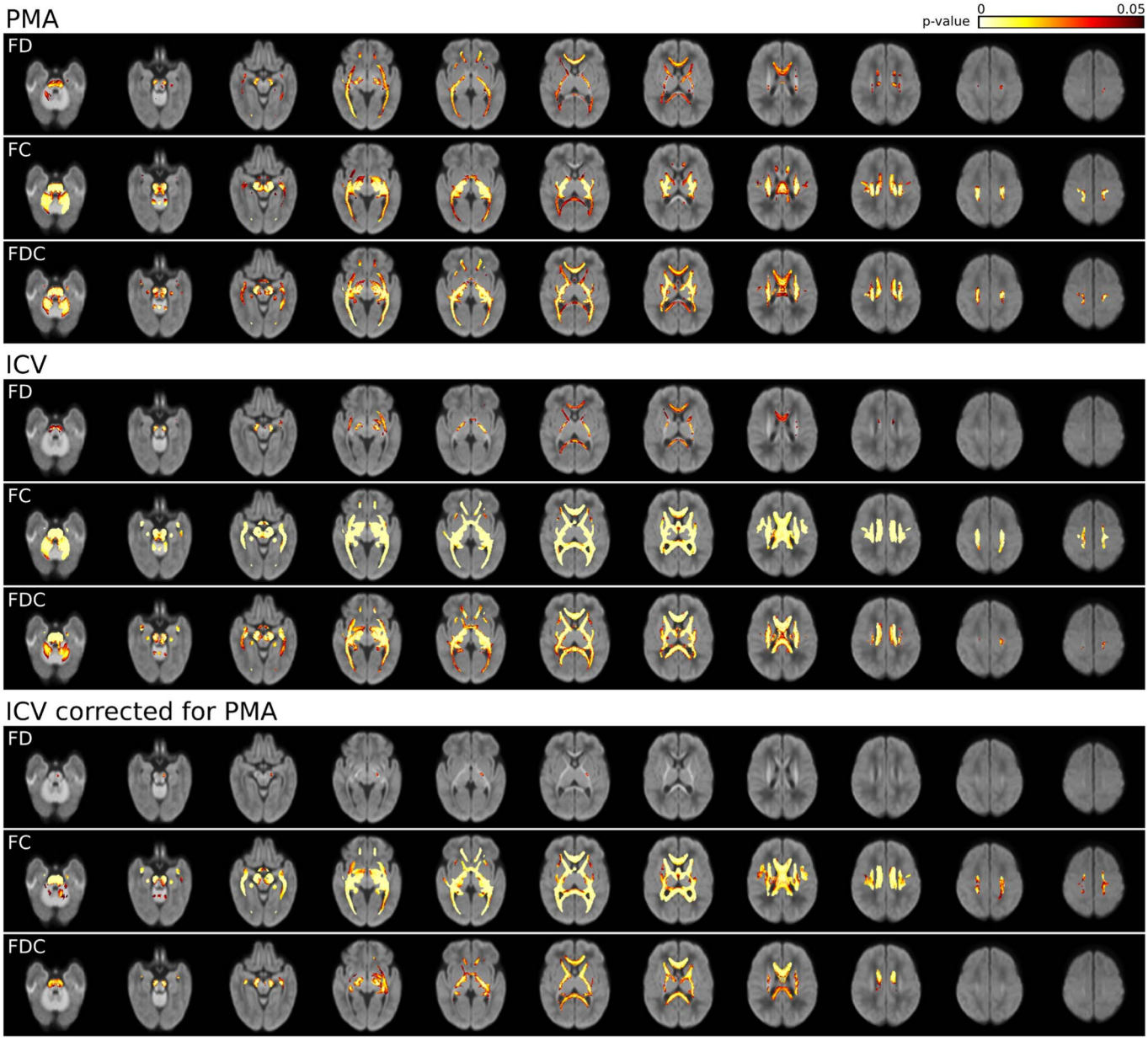

Fig. 2. Correlation between fixel metrics and postmenstrual age (PMA) and intracranial volume (ICV). p-values are overlaid on the total voxelwise FD map. FD, FC, and FDC are positively correlated with PMA and ICV. The correlation between FC and FDC and ICV remains significant throughout the brain when correcting for PMA.

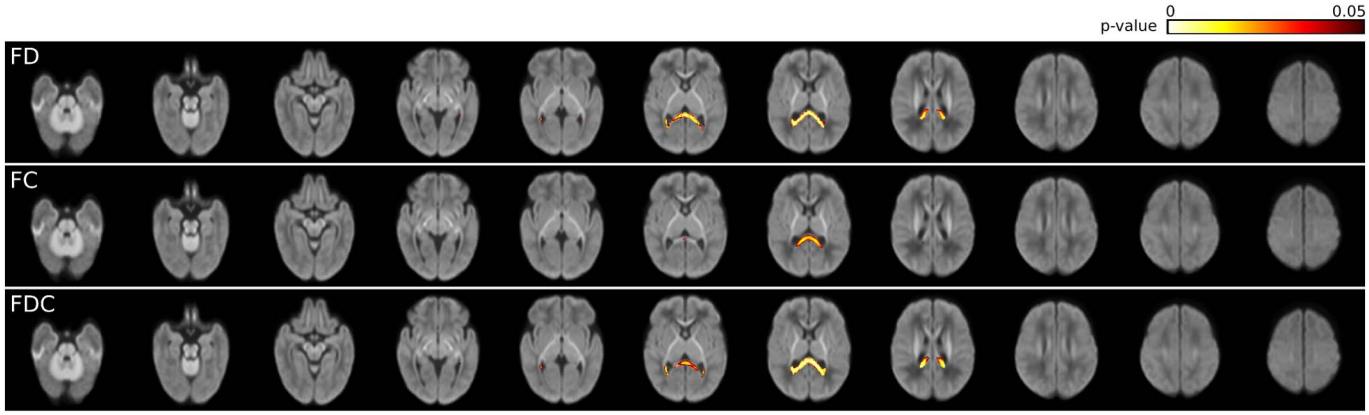

Fig. 3. Correlation between fixel metrics and gestational age (GA) at birth. p-values are overlaid on the total voxelwise FD map. FD, FC, and FDC are positively correlated with GA in the splenium of the corpus callosum. For all measurements, PMA was included as a confounding variable. For FC and FDC, intracranial volume was additionally included as a confounding variable.

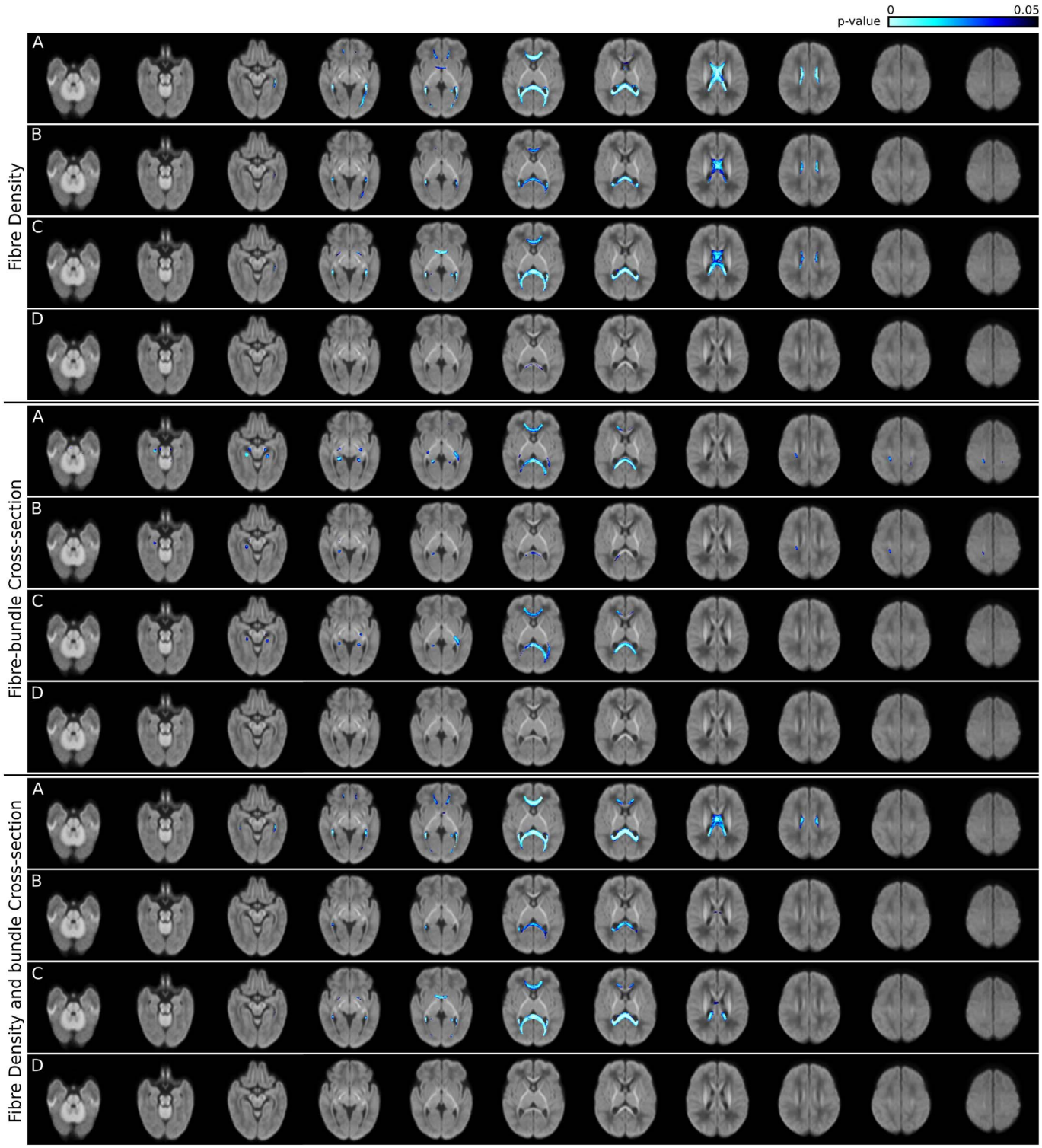

Fig. 4. Comparison between infant groups. p-values are overlaid on the total voxelwise FD map. Top panel: fibre density (FD), middle panel: fibre cross-section (FC), bottom panel: fibre density and cross-section (FDC). In each panel: A: preterm infants compared to term-born infants; B: preterm infants with no brain abnormality compared to term-born infants; C: preterm infants with minimal brain abnormality compared to term-born infants; D: preterm infants with minimal brain abnormality compared to preterm infants with no brain abnormality.

of the right fornix. Reductions in FD in these areas in preterm infants *with* minimal brain abnormalities were more spatially extended; in addition, FD was reduced in the anterior commissure extending to the temporal lobes. There was a small area within the splenium of the corpus callosum that showed statistically significant differences in FD in preterm infants *without* brain abnormalities compared to preterm infants *with* minimal brain abnormalities.

3.4.2.2. Fibre density and bundle cross-section (FDC). In preterm infants *without* brain abnormalities, FDC was reduced compared to term-born infants in the splenium of the corpus callosum, and a small area of the midbody of the corpus callosum. Preterm infants *with* minimal brain abnormalities had reduced FDC compared to term-born infants in the genu of the corpus callosum, the splenium of the corpus callosum, and the anterior commissure. There were no statistically significant

differences in FDC between preterm infants *without* brain abnormality and those *with* minimal brain abnormality.

3.4.2.3. Fibre-bundle cross-section (FC). In preterm infants *without* brain abnormality compared to term-born infants, FC was reduced in the right cerebral peduncle, the right cingulum bundle in the temporal lobe, the splenium of the corpus callosum, and the white matter of the right postcentral gyrus. In contrast, in preterm infants *with* minimal brain abnormality, FC was reduced compared to term-born infants in the left cerebral peduncle, the cingulum bundle in the temporal lobes bilaterally, the left optic radiation, and the genu and splenium of the corpus callosum. There were no statistically significant differences in FC between preterm infants *without* brain abnormality and those *with* minimal brain abnormality.

4. Discussion

To our knowledge, this is the first study to employ a fixel-based analysis in preterm-born infants at term equivalent age. In contrast to previous studies using voxel-based analyses of diffusion tensor imaging (DTI) measures such as fractional anisotropy (FA) or mean diffusivity (MD), fixel-based analysis is based on a model that is able to resolve crossing fibres, and performs statistical analysis for the individual fibre populations in the voxel (fixel). In addition, fixel based analysis allows the assessment of both tissue microstructure (FD), local macrostructure (FC), and the interaction between microstructure and macrostructure (FDC). We found that measures of FD, FC, and FDC were correlated with gestational age at birth, and showed differences between preterm-born infants and term-born infants. Postmenstrual age at the time of MRI was identified as a confounding variable for all measures. In addition, intracranial volume was identified as a confounding variable for FC and FDC.

Postmenstrual age (PMA) at the time of MRI was significantly positively correlated with FD, FC, and FDC. At term equivalent age, the majority of axons are already laid down, with myelination ongoing. Increasing myelination causes the axons to be pushed apart (Fig. 5); the more myelinated, the greater the spatial extent taken up by the fibre bundle and the higher the FC. We would expect to observe a *decrease* in FD, because there are now fewer axons present in each voxel. Our experiments, however, showed an increase in FD. A possible explanation is that the exchange rate between intra-axonal and extra-axonal spaces are reduced due to the increasing myelination, causing an apparent increase in the intra-axonal compartment (Cohen and Assaf, 2010), and hence an increase in FD (Fig. 5). An increase in the intra-axonal compartment has previously been observed using NODDI in young children (Jelescu et al., 2015).

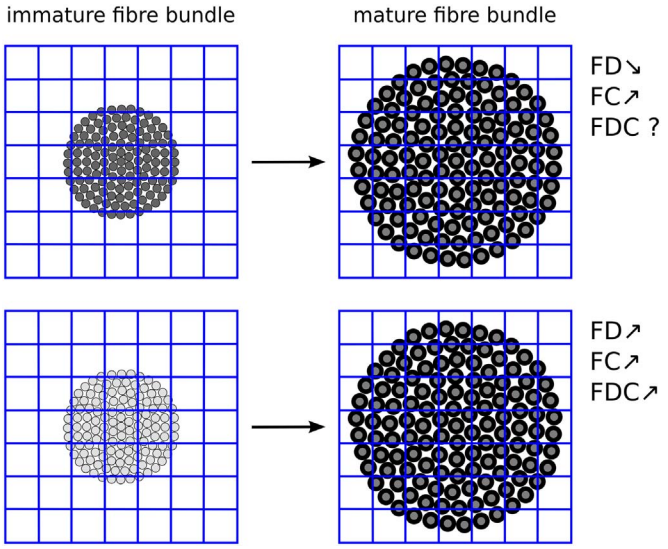

Fig. 5. Changes in fixel measures during brain development. Grey circles indicate axons (grey level indicates degree of diffusion restriction), black circumference indicates myelination. As myelination increases, axons are pushed further apart. Top: If myelination does not affect the diffusion restriction, a decrease in FD is expected, together with an increase in FC. Bottom: If myelination increases diffusion restriction (potentially due to a slowing in the exchange rate between intra-axonal and extra-axonal space), an increase in FD could be observed.

All assessed measures (FD, FC, and FDC) showed a significant positive correlation with gestational age at birth within the splenium of the corpus callosum. This result indicates that the splenium of the corpus callosum is altered both microstructurally and macrostructurally with increased prematurity. On the other hand, FD, FC, and FDC were reduced in preterm-born infants compared to term-born infants in a number of brain regions. While FD and FDC showed largely overlapping patterns of reduction, decreases in FC were also seen in brain regions that showed no alterations in FD or FDC (Fig. 4); conversely, not all areas showing reductions in FD or FDC showed alterations in FC. This finding highlights that these measures provide complementary information: FD is thought to be related to microstructural properties of the white matter, whereas FC pertains to macrostructural properties (cross-sectional area). Alterations in brain microstructure and brain macrostructure can occur in conjunction, or independently. We found that both brain microstructure (i.e. FD) and brain macrostructure (i.e. FC) were altered in the genu and splenium of the corpus callosum; on the other hand, brain microstructure - but not macrostructure - was altered within the body of the corpus callosum, and brain macrostructure - but not microstructure - was altered within the cerebral and cerebellar peduncles, the cingulum bundle (within the temporal lobes), and the optic radiations. We also identified reduced FD, but not FC, in preterm infants in the anterior commissure; however, as discussed by Raffelt and colleagues, the relatively coarse resolution of the acquired diffusion MRI data leads to partial volume effects in this thin white matter structure, thereby making alterations in FD and FC difficult to differentiate (Raffelt et al., 2016).

The FDC was reduced only in areas that also demonstrated reductions in FD, including (but not restricted to) those overlapping with FC reductions (Fig. 4). FDC is a combined measure of FD and FC (multiplicative), and is therefore influenced by both brain microstructural and macrostructural properties. It is thought that FDC is “more likely to reflect differences in ‘the ability to relay information’ compared to fibre density or fibre-bundle cross section alone” (Raffelt et al., 2016). In preterm infants, FDC was reduced in the genu, posterior midbody, isthmus, and splenium of the corpus callosum, compared to term-born infants.

The observed changes with gestational age at birth, as well as the observed decreases in preterm compared to term born infants, may be caused either by decreased myelination, a reduced axon number, or both. Further research, including postmortem histology studies, is required to establish the relationship between physiological tissue changes and fixel metrics.

Preterm-born infants in this study were selected from a larger cohort: only infants with no or only minimal brain abnormality (based on the scoring system of Kidokoro et al. with modified cut-points (Kidokoro et al., 2013; George et al., 2017)) were selected. We subsequently dichotomised the preterm infant group based on their MRI scores for the domains of the scoring system: (i) those infants who showed no abnormality in any of the domains, and (ii) those who showed mild-to-moderate abnormality in at least one of the domains (termed infants with minimal brain abnormality). Preterm infants with minimal brain abnormality showed larger regions of reduced FD, FC, and FDC than did preterm infants without brain abnormality; as expected within the same regions reported above for the comparison of all preterm infants and term-born infants. When comparing preterm infants with and without minimal brain injury directly, however, there were little statistically significant differences between the two groups:

FD was slightly reduced in a small area of the splenium of the corpus callosum. It should be noted that infants with minimal brain abnormality had mixed appearances (see Table 2 and Supplementary material): 3 infants had white matter abnormality, 7 had deep grey matter abnormality, 6 had cortical grey matter abnormality, 5 had cerebellar abnormality, and 5 had abnormalities in multiple domains. Considering this mixed phenotype, as well as the relatively small sample size (29 infants without brain abnormality, 26 with minimal brain abnormality), it is perhaps not surprising that no differences were observed. Future research will investigate more selective subgroups (e.g. infants with only white matter abnormalities of increasing severity), however a larger sample size will be required.

In this study, we limited inclusion of infants to those with no or only minimal brain abnormality. We expect that infants with more severe brain abnormalities would show further reduced FD, FC, and FDC; however, these infants were excluded from the current study a priori, because severe brain abnormalities may influence the accuracy of the image registration that is required for fixel-based analysis. We also only included MRIs acquired around term-equivalent age. Preterm infants were scanned on two occasions: early in life (between 29 and 35 weeks postmenstrual age) and again at term-equivalent age. The preterm brain develops rapidly, progressing from a relatively smooth appearance of the cortex to a highly folded cortex; furthermore, during early brain development, the cortex shows a radial organisation, that can be observed with diffusion MRI (McKinstry et al., 2002). Both factors impact on the accuracy of the image registration, and need to be addressed in detail before fixel-based analysis can be applied to preterm infants scanned early in life. While we acquired diffusion data at 2 b-values (30 directions at b = 1000 s/mm^2 and 64 directions at b = 2000 s/mm^2), in this study we only used the high b-value data for fixel-based analysis. Multi-shell data can be used in the estimation of fibre orientations using constrained spherical deconvolution (Jeurissen et al., 2014), which provides the advantage of separating tissue types; however, efforts to validate this method for the neonate brain are still ongoing (Pietsch et al., 2017). In comparison to adult HARDI data (typical b-value of 3000 s/mm^2), our b-value of 2000 s/mm^2 is relatively low. At this lower b-value, the suppression of extra-cellular water may still be incomplete, which may impact the fixel measures. In the neonate brain, the signal intensity of diffusion weighted images is lower than in the adult brain, due to the higher water content and lower myelination. A b-value of 2000 s/mm^2 was used in this study as a trade-off between angular resolution and suppression of extra-axonal water, and signal-to-noise ratio. Finally, in this study we did not investigate the relationship between the fixel-based measures and neurodevelopmental outcome. Infants enrolled in this study are followed up with detailed neurodevelopmental, neurobehavioural, and neurological assessments until corrected age 2 years, with data collection still ongoing. Future research will investigate whether fixel-based measures are correlated with neurodevelopmental outcomes, and are suitable biomarkers for prediction of outcomes.

5. Conclusion

We demonstrated that fixel-based analysis in preterm-born infants at term equivalent age can be used to identify brain regions of altered white matter development or injury. Brain regions included those associated with functions known to be adversely affected in preterm individuals. Future research will investigate whether fixel-based measures are directly linked with neurodevelopmental outcomes.

Supplementary data to this article can be found online at https://doi.org/10.1016/j.nicl.2018.01.003.

Acknowledgements

Funding: This work was supported by grants from the Cerebral Palsy Alliance Research Foundation (IRG1413), the Financial Markets Foundation for Children (2014-074), and the Queensland Government (Smart State; Health Practitioner Stimulus Grant). The authors received funding from the University of Queensland (University of Queensland Research Scholarship [JMG]), the Queensland Government (Smart State PhD Top-Up Scholarship [JMG]), and the National Health and Medical Research Council (Research Fellowship RF 1105038 [RNB]).

We would like to acknowledge the families of infants who participated in this study, the medical and nursing staff of the neonatal unit, radiology and administrative staff in the department of medical imaging, and research nurses who undertake recruitment and study management.

References

Akazawa, K., Chang, L., Yamakawa, R., Hayama, S., Buchthal, S., Alicata, D., Andres, T., Castillo, D., Oishi, K., Skranes, J., Ernst, T., Oishi, K., 2015. Probabilistic maps of the white matter tracts with known associated functions on the neonatal brain atlas: application to evaluate longitudinal developmental trajectories in term-born and preterm-born infants. NeuroImage 128, 167–179. http://dx.doi.org/10.1016/j.neuroimage.2015.12.026.

Allen, M.C., Cristofalo, E.A., Kim, C., 2011. Outcomes of preterm infants: morbidity replaces mortality. Clin. Perinatol. 38 (3), 441–454. http://dx.doi.org/10.1016/j.clp.2011.06.011.

Braga, R.M., Roze, E., Ball, G., Merchant, N., Tusor, N., Arichi, T., Edwards, D., Rueckert, D., Counsell, S.J., 2015. Development of the corticospinal and callosal tracts from extremely premature birth up to 2 years of age. PLoS One 10 (5), e0125681. http://dx.doi.org/10.1371/journal.pone.0125681.

Cohen, Y., Assaf, Y., 2010. Extracting geometric properties of white matter with q-space diffusion MRI. In: Diffusion MRI: Theory, Methods, and Applications, pp. 125–151.

Dubois, J., Dehaene-Lambertz, G., Perrin, M., Mangin, J.F., Cointepas, Y., Duchesnay, E., Le Bihan, D., Hertz-Pannier, L., 2008. Asynchrony of the early maturation of white matter bundles in healthy infants: quantitative landmarks revealed noninvasively by diffusion tensor imaging. Hum. Brain Mapp. 29 (1), 14–27. http://dx.doi.org/10.1002/hbm.20363.

Eaton-Rosen, Z., Melbourne, A., Orasanu, E., Cardoso, M.J., Modat, M., Bainbridge, A., Kendall, G.S., Robertson, N.J., Marlow, N., Ourselin, S., 2015. Longitudinal measurement of the developing grey matter in preterm subjects using multi-modal MRI. NeuroImage 111, 580–589. http://dx.doi.org/10.1016/j.neuroimage.2015.02.010.

Gao, J., Li, X., Li, Y., Zeng, L., Jin, C., Sun, Q., Xu, D., Yu, B., Yang, J., 2016. Differentiating T2 hyperintensity in neonatal white matter by two-compartment model of diffusional kurtosis imaging. Sci. Rep. 6, 24473. http://dx.doi.org/10.1038/srep24473.

George, J.M., Boyd, R.N., Colditz, P.B., Rose, S.E., Pannek, K., Fripp, J., Lingwood, B.E., Lai, M.M., Kong, A.H., Ware, R.S., Coulthard, A., Finn, C.M., Bandaranayake, S.E., 2015. PPREMO: a prospective cohort study of preterm infant brain structure and function to predict neurodevelopmental outcome. BMC Pediatr. 15, 123. http://dx.doi.org/10.1186/s12887-015-0439-z.

George, J.M., Fiori, S., Fripp, J., Pannek, K., Bursle, J., Moldrich, R.X., Guzzetta, A., Coulthard, A., Ware, R.S., Rose, S.E., Colditz, P.B., Boyd, R.N., 2017. Validation of an MRI brain injury and growth scoring system in very preterm infants scanned at 29- to 35-week postmenstrual age. AJNR Am. J. Neuroradiol. 38 (7), 1435–1442. http://dx.doi.org/10.3174/ajnr.A5191.

Hasan, K.M., Kamali, A., Kramer, L.A., Papnicolaou, A.C., Fletcher, J.M., Ewing-Cobbs, L., 2008. Diffusion tensor quantification of the human midsagittal corpus callosum subdivisions across the lifespan. Brain Res. 1227, 52–67. http://dx.doi.org/10.1016/j.brainres.2008.06.030.

Jelescu, I.O., Veraart, J., Adisetiyo, V., Milla, S.S., Novikov, D.S., Fieremans, E., 2015. One diffusion acquisition and different white matter models: how does microstructure change in human early development based on WMTI and NODDI? NeuroImage 107, 242–256. http://dx.doi.org/10.1016/j.neuroimage.2014.12.009.

Jeurissen, B., Leemans, A., Tournier, J.D., Jones, D.K., Sijbers, J., 2013. Investigating the prevalence of complex fiber configurations in white matter tissue with diffusion magnetic resonance imaging. Hum. Brain Mapp. 34 (11), 2747–2766. http://dx.doi.org/10.1002/hbm.22099.

Jeurissen, B., Tournier, J.D., Dhollander, T., Connelly, A., Sijbers, J., 2014. Multi-tissue constrained spherical deconvolution for improved analysis of multi-shell diffusion MRI data. NeuroImage 103, 411–426. http://dx.doi.org/10.1016/j.neuroimage.2014.07.061.

Kersbergen, K.J., Leemans, A., Groenendaal, F., van der Aa, N.E., Viergever, M.A., de Vries, L.S., Benders, M.J., 2014. Microstructural brain development between 30 and 40 weeks corrected age in a longitudinal cohort of extremely preterm infants. NeuroImage 103, 214–224. http://dx.doi.org/10.1016/j.neuroimage.2014.09.039.

Kidokoro, H., Neil, J.J., Inder, T.E., 2013. New MR imaging assessment tool to define brain abnormalities in very preterm infants at term. AJNR Am. J. Neuroradiol. 34 (11), 2208–2214. http://dx.doi.org/10.3174/ajnr.A3521.

Kidowaki, S., Morimoto, M., Yamada, K., Sakai, K., Zuiki, M., Maeda, H., Yamashita, S., Morita, T., Hasegawa, T., Chiyonobu, T., Tokuda, S., Hosoi, H., 2016. Longitudinal change in white matter in preterm infants without magnetic resonance imaging abnormalities: assessment of serial diffusion tensor imaging and their relationship to neurodevelopmental outcomes. Brain Dev. 39 (1), 40–47. http://dx.doi.org/10.1016/j.braindev.2016.07.007.

Lebel, C., Gee, M., Camicioli, R., Wieler, M., Martin, W., Beaulieu, C., 2012. Diffusion tensor imaging of white matter tract evolution over the lifespan. NeuroImage 60 (1), 340–352. http://dx.doi.org/10.1016/j.neuroimage.2011.11.094.

Manjón, J.V., Coupé, P., Concha, L., Buades, A., Collins, D.L., Robles, M., 2013. Diffusion weighted image denoising using overcomplete local PCA. PLoS One 8 (9), e73021. http://dx.doi.org/10.1371/journal.pone.0073021.

McKinstry, R.C., Mathur, A., Miller, J.H., Ozcan, A., Snyder, A.Z., Schefft, G.L., Almli, C.R., Shiran, S.I., Conturo, T.E., Neil, J.J., 2002. Radial organization of developing preterm human cerebral cortex revealed by non-invasive water diffusion anisotropy MRI. Cereb. Cortex 12 (12), 1237–1243.

Morris, D., Nossin-Manor, R., Taylor, M.J., Sled, J.G., 2011. Preterm neonatal diffusion processing using detection and replacement of outliers prior to resampling. Magn. Reson. Med. 66 (1), 92–101.

Nossin-Manor, R., Card, D., Morris, D., Noormohamed, S., Shroff, M.M., Whyte, H.E., Taylor, M.J., Sled, J.G., 2013. Quantitative MRI in the very preterm brain: assessing tissue organization and myelination using magnetization transfer, diffusion tensor and T_1 imaging. NeuroImage 64, 505–516. http://dx.doi.org/10.1016/j.neuroimage.2012.08.086.

Pannek, K., Raffelt, D., Bell, C., Mathias, J.L., Rose, S.E., 2012. HOMOR: higher order model outlier rejection for high b-value MR diffusion data. NeuroImage 63 (2), 835–842. http://dx.doi.org/10.1016/j.neuroimage.2012.07.022.

Pannek, K., Fripp, J., George, J., Boyd, R., Colditz, P., Rose, S., 2017. Automatic detection of volumes affected by subvolume movement. In: Proceedings of the 25th Annual Meeting of ISMRM, Honolulu, Hawaii, USA, pp. 1786.

Pietsch, M., Hutter, J., Price, A., Kuklisova Murgasova, M., Hughes, E., Steinweg, J., Tusor, N., Andersson, J., Bastiani, M., Sotiropoulos, S., Hajnal, J.V., Tournier, J.D., 2017. Multi-shell neonatal brain HARDI template. In: Proceedings of the 25th Annual Meeting of ISMRM, Honolulu, Hawaii, USA, pp. 1268.

Raffelt, D., Tournier, J.D., Fripp, J., Crozier, S., Connelly, A., Salvado, O., 2011. Symmetric diffeomorphic registration of fibre orientation distributions. NeuroImage 56 (3), 1171–1180. http://dx.doi.org/10.1016/j.neuroimage.2011.02.014.

Raffelt, D., Tournier, J.D., Crozier, S., Connelly, A., Salvado, O., 2012. Reorientation of fiber orientation distributions using apodized point spread functions. Magn. Reson. Med. 67 (3), 844–855. http://dx.doi.org/10.1002/mrm.23058.

Raffelt, D.A., Smith, R.E., Ridgway, G.R., Tournier, J.D., Vaughan, D.N., Rose, S., Henderson, R., Connelly, A., 2015. Connectivity-based fixel enhancement: whole-brain statistical analysis of diffusion MRI measures in the presence of crossing fibres. NeuroImage 117, 40–55. http://dx.doi.org/10.1016/j.neuroimage.2015.05.039.

Raffelt, D.A., Tournier, J.D., Smith, R.E., Vaughan, D.N., Jackson, G., Ridgway, G.R., Connelly, A., 2016. Investigating white matter fibre density and morphology using fixel-based analysis. NeuroImage. http://dx.doi.org/10.1016/j.neuroimage.2016.09.029.

Rose, J., Vassar, R., Cahill-Rowley, K., Guzman, X.S., Stevenson, D.K., Barnea-Goraly, N., 2014. Brain microstructural development at near-term age in very-low-birth-weight preterm infants: an atlas-based diffusion imaging study. NeuroImage 86, 244–256. http://dx.doi.org/10.1016/j.neuroimage.2013.09.053.

Saigal, S., Doyle, L.W., 2008. An overview of mortality and sequelae of preterm birth from infancy to adulthood. Lancet 371 (9608), 261–269. http://dx.doi.org/10.1016/S0140-6736(08)60136-1.

Shi, J., Chang, L., Wang, J., Zhang, S., Yao, Y., Zhang, S., Jiang, R., Guo, L., Guan, H., Zhu, W., 2016. Initial application of diffusional kurtosis imaging in evaluating brain development of healthy preterm infants. PLoS One 11 (4), e0154146. http://dx.doi.org/10.1371/journal.pone.0154146.

Tournier, J.D., Calamante, F., Connelly, A., 2007. Robust determination of the fibre orientation distribution in diffusion MRI: non-negativity constrained super-resolved spherical deconvolution. NeuroImage 35 (4), 1459–1472. http://dx.doi.org/10.1016/j.neuroimage.2007.02.016.

Tournier, J., Calamante, F., Connelly, A., 2012. MRtrix: diffusion tractography in crossing fiber regions. Int. J. Imaging Syst. Technol. 22 (1), 53–66.

Volpe, J.J., 2009. The encephalopathy of prematurity—brain injury and impaired brain development inextricably intertwined. Semin. Pediatr. Neurol. 16 (4), 167–178. http://dx.doi.org/10.1016/j.spen.2009.09.005.

Wu, D., Chang, L., Akazawa, K., Oishi, K., Skranes, J., Ernst, T., Oishi, K., 2017. Mapping the critical gestational age at birth that alters brain development in preterm-born infants using multi-modal MRI. NeuroImage. http://dx.doi.org/10.1016/j.neuroimage.2017.01.046.